

## THE ROLE OF GRAIL ORBIT DETERMINATION IN PREPROCESSING OF GRAVITY SCIENCE MEASUREMENTS

**Gerhard Kruizinga\*, Sami Asmar\*, Eugene Fahnestock\*, Nate Harvey\*, Daniel Kahan\*, Alex Konopliv\*, Kamal Oudrhiri\*, Meegyeong Paik\*, Ryan Park\*, Dmitry Strelakov\*, Michael Watkins\* and Dah-Ning Yuan\***

The Gravity Recovery And Interior Laboratory (GRAIL) mission has constructed a lunar gravity field with unprecedented uniform accuracy on the farside and nearside of the Moon. GRAIL lunar gravity field determination begins with preprocessing of the gravity science measurements by applying corrections for time tag error, general relativity, measurement noise and biases. Gravity field determination requires the generation of spacecraft ephemerides of an accuracy not attainable with the pre-GRAIL lunar gravity fields. Therefore, a bootstrapping strategy was developed, iterating between science data preprocessing and lunar gravity field estimation in order to construct sufficiently accurate orbit ephemerides. This paper describes the GRAIL measurements, their dependence on the spacecraft ephemerides and the role of orbit determination in the bootstrapping strategy. Simulation results will be presented that validate the bootstrapping strategy followed by bootstrapping results for flight data, which have led to the latest GRAIL lunar gravity fields.

### INTRODUCTION

The twin Gravity Recovery and Interior Laboratory (GRAIL) spacecraft were launched from Cape Canaveral on 10 September 2012 and were inserted into lunar orbit on 31 December 2011 and 01 January 2012. During the science phase the GRAIL spacecraft flew in formation in nearly identical orbits with separation distances varying between 30 and 200 km. The objective of the GRAIL mission was to measure a high resolution lunar gravity field using inter-satellite range measurements, a mission design pioneered by the Gravity Recovery and Climate Experiment (GRACE).<sup>1</sup> The high resolution lunar gravity field generated will be used by the GRAIL science team to investigate the formation evolution of the Moon from crust to the deep interior.<sup>2</sup> Science measurements were collected during the primary mission from 01 March 2012 until 29 May 2012 and the extended mission from 30 August 2012 until 14 December 2012. In the primary mission the twin spacecraft flew at orbital altitudes from 30 to 100 km and at separations from 60 to 200 km. In the extended mission the average orbital altitude was lowered to 25 km, however in the last month of operations the orbital altitude was lowered again, with altitudes as low as 2 km above the lunar surface. The spacecraft separation was reduced to 50 km in the extended mission and to 40 km in the last month to reduce multipath signal from the lunar surface for the inter-satellite ranging system.

The main science instrument on each GRAIL spacecraft was the Lunar Gravity Ranging System (LGRS), which used a carrier-only radio link between the two spacecraft at Ka-band frequency.

---

\*Jet Propulsion Laboratory, California Institute of Technology, 4800 Oak Grove Drive, Pasadena CA 91109

The LGRS Ka-carrier frequency and the LGRS (science) timing clock were derived from an Ultra Stable Oscillator (USO). The same USO was used by the Time Transfer System (TTS) to generate ranging code modulated on an S-band carrier between the two spacecraft. The TTS pseudorange measurements were used to compute the relative clock offset of the two LGRS clocks, to ensure that the Ka ranging accuracy requirement was achieved. The twin spacecraft also had a carrier-only Radio Science Beacon (RSB) at X-band, again derived from the USO. The RSB signal served two purposes. First, the RSB is used to measure the USO frequency, which was used to scale the LGRS Ka carrier range measurement. Second, the RSB one-way X-band data is used as a tracking data type in the orbit determination process. Finally, both spacecraft used an S-band signal for telecommunication and to transmit navigation radiometric tracking data to the DSN stations.

Absolute timing on GRAIL requires coordination of three onboard clocks: LGRS, BTC and RTC. Providing absolute timing for the GRAIL science measurements was a challenge because absolute timing measurements could only be made when the spacecraft were on the nearside of the Moon and being tracked by a DSN station. Furthermore, the LGRS (science) clocks were free running clocks and not tied to any other clock, and LGRS clock time tags were set to zero after each LGRS boot up. In the GRAIL timing design time correlation measurements were made between the LGRS clock and the onboard Base Time Clock (BTC). The BTC in turn was correlated with an onboard software-generated Real Time Clock (RTC) with measurements provided by the onboard processor. The RTC was then correlated with Coordinated Universal Time (UTC) at a DSN station using time correlation packets transmitted via S-band telecommunication. Each of the time correlations in the absolute GRAIL timing design had unknown instrument biases and limited precision. Fortunately, twice per month favorable orbit geometry allowed a unbiased and precise measurement of the absolute LGRS clock by eavesdropping on the ranging signal of the TTS at a DSN station.

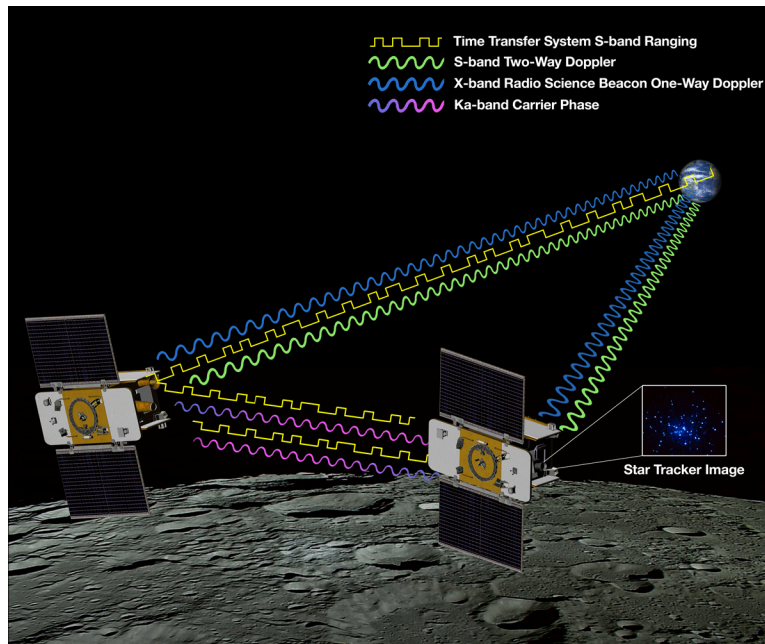


**Figure 1:** GRAIL gravity science measurements

The GRAIL measurements processed during lunar gravity field estimation (depicted in Figure 1) are:

- Inter-satellite Ka-band carrier phase measurements by the LGRS. Combination of the Ka phase measurements in each direction results in inter-satellite range measurements, the primary GRAIL science product.
- Inter-satellite pseudo range and phase measurements at S-band generated by the Time Transfer System (TTS). Subtracting the pseudo measurements in each direction determines the relative clock alignment of the LGRS (science) clocks.
- Two-Way S-band Doppler tracking data of the GRAIL telecommunication system at the Deep Space Network (DSN). Used in orbit determination.
- One-Way X-band Doppler tracking data of the GRAIL Radio Science Beacon (RSB) at the DSN. Used during orbit determination and determination of the USO frequency, needed to form the inter satellite-range measurements.
- Star tracker GRAIL spacecraft attitude quaternion measurements. Used in orbit determination and inter-satellite range corrections.
- Time correlation packet absolute timing measurement sent over the GRAIL S-band telecommunication link. Provides a time correlation between Coordinated Universal Time (UTC) and spacecraft clock.
- Pseudorange measurement of TTS link at DSN station when GRAIL orbit geometry is favorable. Provides a direct time correlation between the LGRS (science) clocks and UTC.

Before the Lunar gravity field determination process can begin, the GRAIL science measurements are transformed into the Solar System Barycentric Frame (SSBF) since JPL's MIRAGE gravity field determination software processes measurements in SSBF. The measurement transformations include corrections for general relativity, timing and satellite motion in SSBF. All these measurement transformations depend directly or indirectly on the spacecraft ephemerides. The primary measurement for GRAIL is the inter-satellite range, which requires transformations with sub- $\mu\text{m}$  accuracy. To meet this accuracy requirement, the spacecraft ephemerides accuracy needs to be less than 1 m. For orbital altitudes less than 100 km, orbit determination with pre-GRAIL lunar gravity models can only achieve spacecraft ephemerides accuracies at the 300 m level, because the pre-GRAIL Lunar gravity fields do not contain gravity information on the deep far side of the Moon and no DSN tracking data is available on the deep far side, which always points away from Earth. Therefore, preprocessing of GRAIL science measurements needs to include improvement of the gravity field, to meet the accuracy requirements for the measurement transformations. This was achieved for GRAIL by developing a bootstrapping strategy, where the relative orbit ephemerides accuracy was first improved by including inter-satellite range rate observations in the orbit determination process. After a gravity field update, the focus shifted to improving DSN tracking data fits, timing of the GRAIL measurements and inter-satellite range corrections, followed by another gravity field update. This latter process was continued until convergence.

This paper describes the role of orbit determination in computing the GRAIL measurement transformations and the iterative bootstrapping process needed to improve the Lunar gravity field and the measurement transformations. A full description will be presented of the dependence of all measurements and transformations to SSBF on spacecraft ephemerides. Furthermore, a description of the lunar gravity field determination bootstrapping problem will be given, and a description of

the strategy chosen to solve that problem. Simulation results will be presented, to demonstrate the validity of the bootstrapping strategy solution. Finally, results will be presented for GRAIL flight data.

## GRAIL MEASUREMENT TRANSFORMATIONS TO THE SOLAR SYSTEM BARYCENTRIC FRAME

The objective of the following subsections is to give a generic description of the GRAIL measurement transformations and their dependence on the spacecraft ephemerides. The interested reader can find more complete details in the cited references. Throughout these subsections:

- $\rho$  : Range between two positions
- $\tau$  : Light time between two positions
- $r$  : Position vectors of the twin spacecraft with respect to the Moon-centered SSBF
- $R$  : Position vectors of the twin spacecraft with respect to the SSBF

### Relative Timing of Science Data

The difference between the two LGRS (science) clocks, also known as the relative timing alignment, plays an important role in forming the inter-satellite Dual One Way Range (DOWR) measurement. The GRAIL Ka-band phase measurements are the difference of the outgoing Ka carrier phase and the incoming Ka carrier phase. Adding the Ka-band phase measurements of both spacecraft eliminates most LGRS clock errors, provided the LGRS clocks are aligned better than  $10^{-7}$ s in a bias sense, with a variability about this bias less than  $90 \times 10^{-12}$  s.<sup>3</sup> After aligning the LGRS clocks, the DOWR  $\rho_{dowr}(t)$  is formed at Barycentric Dynamical Time (TDB)  $t$  according to:<sup>3</sup>

$$\rho_{dowr}(t) \equiv c \frac{\phi_1(t) + \phi_2(t)}{f_1 + f_2} \quad (1)$$

where  $\phi_1(t)$ ,  $\phi_2(t)$  are the Ka-band phase measurements,  $f_1$ ,  $f_2$  are the Ka-band carrier frequencies and  $c$  is the speed of light.

The LGRS clocks on the GRAIL twin spacecraft are free running clocks, therefore a measurement is needed of the relative LGRS clock alignment, which meets the requirements stated above. For the GRACE mission the clock alignments were derived from Global Positioning System data. On GRAIL a dedicated system, the Time Transfer System (TTS), sends a ranging code in each direction between the twin spacecraft using an S-band carrier, and allows inter-satellite clock alignment.

*Time Transfer System data* The LGRS clock alignment measurement is computed by subtracting the pseudorange measured on GRAIL-1 from the pseudorange on GRAIL-2 at the same TDB time  $t$ . The pseudorange measurement includes the actual inter-satellite range and LGRS clock drift. The clock alignment measurement  $O_{12}(t)$  is calculated according to:<sup>3</sup>

$$O_{12}(t) = \frac{1}{2}(\tilde{\rho}_1(t) - \tilde{\rho}_2(t)) - \frac{1}{2}(\dot{t}_2 - \dot{t}_1)\tau \quad (2)$$

where  $\tilde{\rho}_1(t)$ ,  $\tilde{\rho}_2(t)$  are the pseudo range measurements and  $\dot{t}_1, \dot{t}_2$  are the LGRS clock rates with respect to TDB. The inter-satellite light time  $\tau$  in equation (2) is calculated from spacecraft ephemerides calculated during the orbit determination process.

## Absolute Timing of Science Data

For the GRAIL mission only a limited number of absolute timing measurements were available, in contrast to the GRACE mission, where absolute timing measurements are continuously available using the GPS system.<sup>1</sup> The GRAIL absolute timing system relied on time correlations between the LGRS (science) clock and two spacecraft clocks, which in turn were correlated with UTC using time correlation packets<sup>4</sup> which are described below. These time correlation packets were only transmitted once every 10 minutes and measurements could only be made when a DSN station was tracking the spacecraft at S-band. Hence, no absolute timing measurements were available on the deep far side of the Moon or during DSN tracking gaps, which lasted up to 18 hours for either spacecraft. The GRAIL absolute timing system measurements were the result of combining several time correlations together, and each individual time correlation had systematic errors like electronic delays and limited precision. The accuracy of the overall GRAIL absolute timing system was found to be at the 0.01 s level.

In preparation for launch it was realized that a direct absolute timing measurement of the LGRS clock could be made using a DSN station to eavesdrop on the TTS S-band ranging signal. By observing the TTS system directly at the DSN the LGRS clock can be correlated directly to UTC, because the TTS and LGRS use the same clock to time-tag their measurements.<sup>4</sup> The TTS Direct To Earth (TTS-DTE) measurement could only be made for favorable GRAIL lunar orbit geometries with respect to Earth. Favorable orbit geometry occurs only twice during the Moon's orbit around the Earth. Furthermore, dedicated hardware was needed to track the TTS-DTE signal, which limited the TTS-DTE measurements to station DSS-24. The accuracy of the TTS-DTE absolute timing measurement was found to be at the  $10^{-8}$  s level.

The determination of absolute timing for the GRAIL mission is based on the assumption that the GRAIL USOs, which drive the LGRS clocks, are very stable. Based on experience with the GRACE USOs, the clock error offset was modeled as a stochastic second order polynomial.<sup>3</sup> The GRAIL clock error offset model was estimated using least squares, combining the following timing measurements made by the GRAIL system:

- Time correlation packets. These measurements provide a biased measurement of the absolute LGRS clock offset, when in view of a DSN station during a DSN tracking session.
- USO frequency measurements. These measurements provides information about the clock offset drift rate during each DSN session which tracks X-band RSB signal.
- TTS clock offset measurements. These measurements continuously provide information on the LGRS clock difference.
- TTS-DTE ranging measurements. Twice per month these measurements provide a direct measurement of the absolute LGRS clock offset.

*Time Correlation Packets* For each spacecraft the spacecraft clock correlation with respect to UTC is computed from:<sup>4</sup>

$$\tilde{t} = \tilde{t}_{utc} - \epsilon_{delay} - \tau \quad (3)$$

where  $\tilde{t}$  is the inferred UTC LGRS time tag,  $\tilde{t}_{utc}$  is the UTC time tag of reception of the time correlation packet at the DSN station,  $\epsilon_{delay}$  is an unknown electronic spacecraft delay and  $\tau$  equals spacecraft to station light travel time. The light time is calculated based on spacecraft ephemerides

from the orbit determination process. The inferred UTC LGRS time tag becomes more accurate as the spacecraft ephemerides accuracy improves, however, the unknown electronic delay remains, limiting the accuracy of this measurement.

*Ultra Stable Oscillator Frequency Measurements* The USO frequency measurements are based on one-way once per orbit RSB Doppler measurement biases estimated during the orbit determination process. The orbit determination process applies doppler corrections to RSB data for Earth’s atmosphere, Earth orientation, lunar gravity model, spacecraft radiation pressure and general relativity. The residual one-way Doppler bias provides a direct measurement of USO frequency, since the USO is used to generate RSB X-band carrier. These USO frequency measurements will become more accurate as the lunar gravity field, spacecraft ephemerides, and other models improve.

*Time Transfer System Data* In contrast to all other timing measurements, the LGRS clock offset measurements described in equation (2) are continuously available. These measurements do depend on the spacecraft ephemerides (inter-satellite light time), but only weakly since the required correction is small. Nevertheless this measurement will become more accurate when the spacecraft ephemerides accuracy improves.

*Time Transfer System Direct To Earth Data* The TTS-DTE ranging measurement<sup>5</sup> is the only direct absolute timing measurement and is calculated according to:<sup>4</sup>

$$\tilde{t} = \tilde{t}_{utc} - \tau \quad (4)$$

This measurement is very similar to the absolute timing measurement calculation shown in equation (3). The spacecraft electronic delay  $\epsilon_{delay}$ , however, is absent because no spacecraft clocks were involved in the measurement. The TTS-DTE measurements were used to calibrate  $\epsilon_{delay}$ , effectively improving the accuracy of the time correlation packet derived absolute timing. The inferred UTC LGRS time tag  $\tilde{t}$  will become more accurate as the spacecraft ephemerides accuracy improves.

*Timing Transformation to Barycentric Dynamical Time* All the GRAIL timing measurements are made by local clocks, and if the onboard clocks were perfect, the measurements would be time tagged with “proper time.”<sup>6</sup> The transformation from “proper time” to TDB time is computed from general relativity where the the proper time clock rate  $\frac{d\tilde{t}}{dt}$  is dependent on the SSBF velocity of the clock  $v(R)$  and location in the gravity potential  $U(R)$ :<sup>6</sup>

$$\frac{d\tilde{t}}{dt} = 1 - \frac{U(R)}{c^2} - \frac{1}{2} \frac{v(R)^2}{c^2} + L \quad (5)$$

The timing transformations were computed with the Jet Propulsion Laboratory (JPL) orbit determination software MIRAGE. It should be noted that GRAIL specific changes were needed in the MIRAGE software to maintain precision level below 1 micron. All time transformation calculations contain the SSBF spacecraft position vectors ( $R$ ) with magnitudes larger than  $10^{11}$  m, therefore, a standard double precision variable of 16 digits can not capture changes at the 1 micron level. The sensitivity of these time transformations to the spacecraft ephemerides is small, however, so floating point error in spacecraft ephemerides does not interfere with GRAIL timing.

### **One-Way and Two-Way Deep Space Network Doppler Data**

The DSN provides one-way RSB X-band and two-way S-band Doppler tracking, which are the primary data source for GRAIL orbit determination. In the orbit determination process, doppler corrections are applied for Earth’s atmosphere, Earth orientation, lunar gravity model, spacecraft

radiation pressure and general relativity. In the early science phase significant systematic residuals were observed due to gravity and spacecraft radiation pressure model errors, limiting the accuracy of the spacecraft ephemerides. As more inter-satellite ranging data was included in the lunar gravity field solution the Doppler residuals were observed to improve as spacecraft ephemerides improve.

### Inter-satellite Ka Ranging Data

The inter-satellite ranging data are the result of adding the inter-satellite Ka-band phase measurements of both spacecraft as described in equation (1), forming the DOWR  $\rho_{dowr}(t)$ . In this equation the sum of the Ka-band carrier frequencies of both spacecraft serves as the scale factor to generate the DOWR range measurements. The same USO frequency measurements described in the ‘‘Absolute Timing of Science Data’’ section are used to generate the Ka-band carrier frequencies. The lunar gravity determination process requires the transformation of the DOWR measurements into instantaneous inter-satellite range measurements  $\rho(t)$  between the spacecraft Center of Mass (COM) shown in Figure 2. The instantaneous inter-satellite range is computed according to:<sup>3</sup>

$$\rho(t) = \rho_{dowr}(t) + \rho_{tof}(t) + \rho_{geom}(t) + K \quad (6)$$

The second term,  $\rho_{tof}(t)$ , is a range correction to account for satellite motion and general relativity. The third term,  $\rho_{geom}(t)$ , is a geometric range correction dependent on the spacecraft attitude, which accounts for the fact that the Ka phase-center is not located at the spacecraft COM. The constant  $K$  represents an ambiguity in the phase measurements underlying the DOWR measurement. In the following subsections the transformations are described in detail, along with their dependencies on the spacecraft ephemerides.

*Ultra Stable Oscillator Frequency Measurements* The primary purpose of the RSB is to provide DSN X-band measurements, from which the USO frequency can be determined as a function of time. From the USO frequency the Ka-carrier frequency can be calculated because the USO drives on-board generation of Ka-band phase, TTS S-band phase, and RSB X-band phase. As described above the USO frequency is determined during the orbit determination process, hence the USO frequency accuracy is related to spacecraft ephemerides accuracy.

*Time of Flight Correction* The Time Of Flight (TOF) correction consists of two components. The first component corrects for the spacecraft motion during the time between transmission and reception of Ka carrier phase. The second component corrects for general relativistic light path bending as illustrated in Figure 2. The geodesic (relativistic) light paths  $\rho_2^1(t_R)$  and  $\rho_1^2(t_R)$  illustrated in Figure 2 are added the same way as the Ka-band phase measurements to form a computed DOWR  $\rho_{dowrcomp}(t_R)$ :

$$\rho_{dowrcomp}(t_R) = \frac{1}{f_1 + f_2} [f_1 \rho_2^1(t_R) + f_2 \rho_1^2(t_R)] \quad (7)$$

The TOF correction  $\rho_{TOF}(t_R)$  is then computed according to:

$$\rho_{TOF}(t_R) = \rho(t_R) - \rho_{dowrcomp}(t_R) \quad (8)$$

where  $\rho(t_R)$  is the instantaneous Euclidean range at receive time  $t_R$ . It should be noted that the TOF correction accuracy depends strongly on the relative spacecraft ephemerides accuracy for spacecraft motion, and more weakly on light path bending.

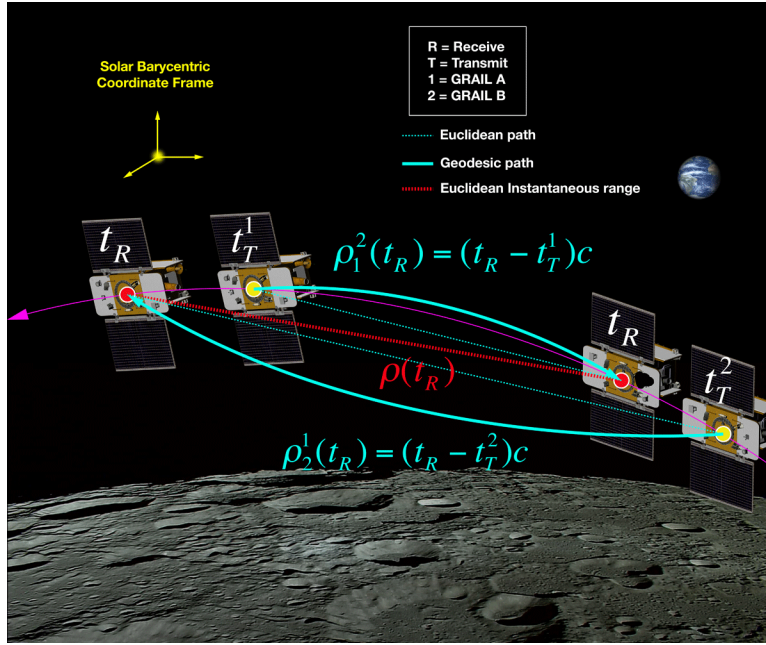


Figure 2: GRAIL Time of Flight Correction Components

*Geometric Range Correction* The objective of the GRAIL mission is to observe the relative motion of the COM of the twin spacecraft. However, the actual measurement is made from Ka phase center to Ka phase center. The vector from the COM to the Ka phase center is called the Ka boresight vector. The Ka boresight vector is shown as the vector L in Figure 3. Ideally the spacecraft should point the Ka boresight vector in the line of sight (LOS) direction to the other spacecraft. During flight this is generally not the case because:

- The pre-flight boresight vector contains errors due to star tracker miss-alignment, COM mislocation and Ka phase center mislocation.
- The boresight vector changes with time as propellant is consumed for maneuvers causing a change in COM.
- The Spacecraft has attitude control errors and onboard LOS vector prediction errors.

Before the geometric range correction can be calculated the LOS vector is calculated from the spacecraft ephemerides according to:

$$LOS = r_2 - r_1 \quad (9)$$

for spacecraft 1. The LOS has the opposite sign when calculated for spacecraft 2. The geometric range correction ( $L\cos\Theta$ ) is then computed as the projection of the Ka boresight vector L on the LOS vector where  $\Theta$  is the angle between the boresight and LOS vector.

The range error due to the spacecraft ephemerides plays a significant role in processing Ka ranging data during special maneuvers designed to estimate the Ka boresight vector. These Ka boresight maneuvers execute a  $3^\circ$  oscillation in yaw and a  $3^\circ$  oscillation in pitch centered on the LOS vector. The Ka boresight vector is estimated by combining the observed range change minima during

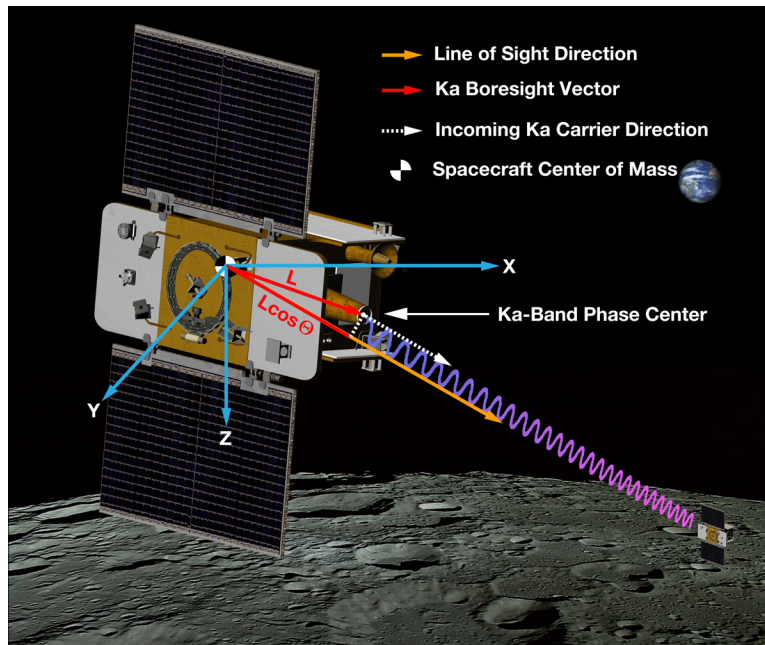


Figure 3: GRAIL Ka Ranging Geometry Correction

these maneuvers. Figure 7a illustrates an example of the range change during a Ka boresight calibration maneuver. During the Ka boresight calibration maneuvers the gravity and orbit geometry range changes can be as large as 1.5 km. In order to detect the 1 mm level range changes caused by the yaw + pitch oscillations, the range signals of the inter-satellite COM movement need to be removed based on spacecraft ephemerides. As the spacecraft ephemerides become more accurate the recovered range change signal improves as well.

### THE LUNAR GRAVITY FIELD DETERMINATION BOOTSTRAPPING PROBLEM

In the previous section the dependence on spacecraft ephemerides for nearly all GRAIL science measurement transformations was discussed. Prior to GRAIL flight it was realized that many of the science measurement transformations would have insufficient accuracy, mainly due to poor knowledge of the pre-flight lunar gravity field. In particular the deep farside of the lunar gravity field knowledge was essentially unknown. The GRAIL project had to solve the problem of estimating the lunar gravity field with science measurements for which the accuracy directly depended on the accuracy of the lunar gravity field used in the data processing. This problem is a classic bootstrapping problem since no other information is available to improve the GRAIL science measurements. In the following subsections the GRAIL bootstrapping strategy is discussed. This is followed by simulation results to validate the GRAIL bootstrapping strategy. Finally, GRAIL flight results from the bootstrapping strategy are presented.

### GRAIL Lunar Gravity Field Determination Bootstrapping Solution Strategy

The initial preparation step of the bootstrapping strategy is to improve the relative spacecraft ephemerides accuracy. When the spacecraft ephemerides are estimated individually in the orbit determination process based on pre-GRAIL lunar fields, the resulting relative spacecraft ephemerides errors are at the 300 m level. The relative spacecraft ephemerides can be improved by including

inter-satellite Ka range rate data. For the orbit determination process the first derivative of the measured inter-satellite range (range rate) is preferred because the errors are more localized. The initial Ka-band inter-satellite range measurement using a pre-flight lunar gravity model is about  $\mathcal{O}(10^2)$  more accurate than the observed relative spacecraft ephemerides error, therefore it can be used as a constraint in the orbit determination process. Furthermore, this measurement is also available on the far side of the Moon allowing relative spacecraft ephemerides improvement for the complete orbit. With the inter-satellite Ka range rate included in the orbit determination process, the relative spacecraft ephemerides errors are reduced to about 3 m with pre-flight lunar gravity models. With relative spacecraft ephemerides accuracy at the 3 m level, the errors in the Time of Flight (TOF) correction for the inter-satellite range are reduced to a few  $\mu\text{m}$ . The spacecraft ephemerides from this initial preparation step are then used to preprocess the GRAIL science measurement again starting the first bootstrapping iteration.

In each bootstrapping iteration the gravity field is adjusted using the DSN Doppler tracking data and improved Ka inter-satellite range rate data. With the adjusted gravity field the absolute spacecraft ephemerides errors are significantly reduced. With the improved spacecraft ephemerides, new timing corrections are estimated and updates are calculated for the Ka-boresight vectors. The science measurement are then preprocessed again with the updated spacecraft ephemerides, timing and Ka-boresight vectors. The bootstrapping iterations are continued until convergence of the gravity field solution, Ka-boresight vectors and timing corrections.

### Simulation Results for GRAIL Gravity Field Determination Bootstrapping Problem

The GRAIL bootstrapping strategy was validated by a comprehensive simulation, which included simulation of GRAIL measurements, DSN tracking data and the complete lunar gravity field determination process. The GRAIL simulation and bootstrapping lunar gravity field determination process is illustrated in Figure 4. The simulation consisted of one month of simulated GRAIL mea-

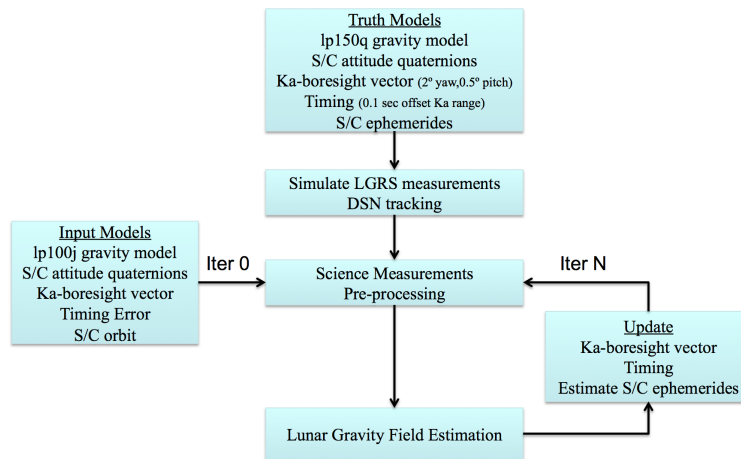


**Figure 4:** GRAIL Simulation and Lunar Gravity Field Determination Bootstrapping Process

surements using the lp150q lunar gravity field<sup>7</sup> as the truth field, a truth inter-satellite Ka range time tag offset from nominal of 0.1 s and truth Ka-boresight vectors offset from nominal by  $2^\circ$  in yaw angle and  $0.5^\circ$  in pitch angle. The bootstrapping strategy was initiated (iteration 0) with the lp100j lunar gravity field,<sup>8</sup> a zero time tag offset for the inter-satellite Ka range time tag and the

nominal Ka-boresight vectors. The lp100j lunar gravity field was chosen under the assumption that the difference with the truth field lp150q would be an upper bound for actual gravity model errors during flight. The simulated Ka-boresight calibration maneuvers were positioned in locations where lp100j high frequency ephemeris errors were at a maximum. The inter-satellite Ka range time tag bias was assumed to be constant over the one month time interval of the simulation.

The Ka-boresight vector and the Ka range time tag error results are shown in Figure 5 for each iteration of the bootstrapping process. It can be seen that at least two iterations are needed to recover both quantities with acceptable remaining errors.

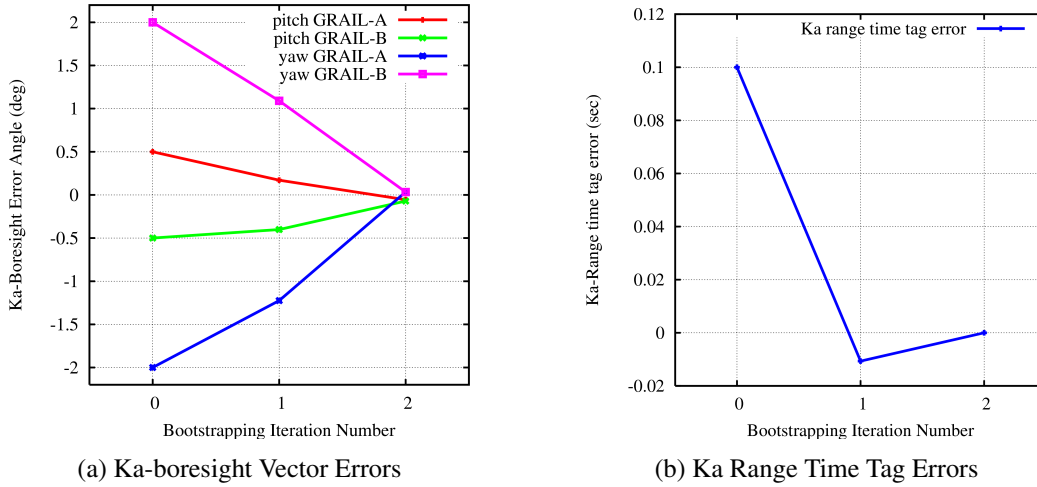


**Figure 5:** Ka-boresight and Ka Range Time Tag Errors Per Bootstrapping Iteration

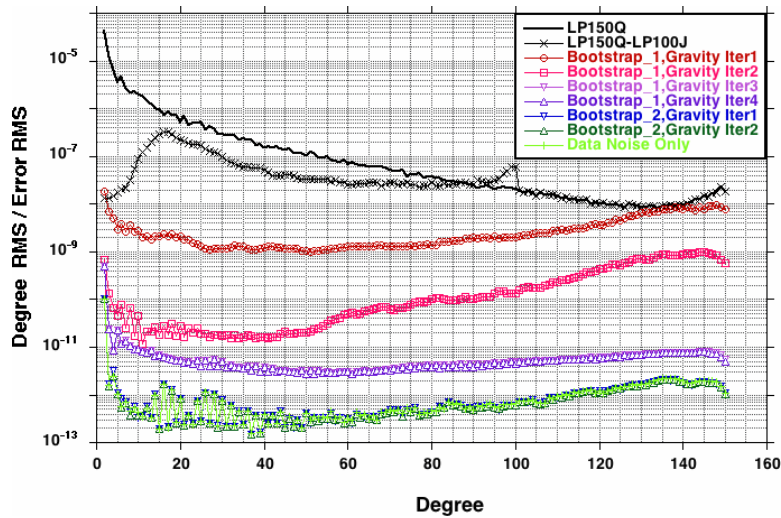


**Figure 6:** Spherical Harmonic Degree/Error RMS Plot for Bootstrapping Simulation Results

The evolution of the recovered lunar gravity fields, during the bootstrapping process, is shown in Figure 6. Figure 6 shows the RMS per degree of the spherical harmonic coefficient values (degree RMS) or the RMS per degree of spherical harmonic difference values (error RMS) with the truth

gravity model lp150q. The total degree RMS for the truth model lp150q is shown for comparison, as is the error RMS of the initial gravity lp100j. It should be noted that since the spherical harmonic coefficients above degree and order are zero for lp100j, the error RMS of lp100j is identical to the degree RMS of lp150q for degrees larger than 100 . Also shown is the error RMS for the “noise only” case where perfect gravity science measurements were processed with data noise based on required instrument performance. The “noise only” case represents the best achievable gravity field.

Within one bootstrapping iteration, the gravity field determination process needs to iterate, which means that the processed science measurements are not reprocessed until the gravity iteration converges. In Figure 6 it can be seen that for the first bootstrapping iteration four gravity iterations were required for convergence. The curves for gravity iteration 3 and 4 are nearly identical and the resulting gravity field error RMS with lp150q is about an order of magnitude larger than the “noise only” case. For the second bootstrapping iteration the gravity science measurements were reprocessed with the gravity field from gravity iteration 4. The two gravity iterations in the second bootstrapping iteration show convergence and the curves are nearly identical to the “noise only” case. Thus the full recovery of the truth lunar gravity lp150q was achieved in two bootstrapping steps, which is consistent with the recovery of the time tag and the Ka-boresight vector.

### **GRAIL Lunar Gravity Field Determination Bootstrapping Flight Results**

The GRAIL lunar gravity field determination bootstrapping strategy was successfully applied on the flight data. However, the first lesson learned for the flight data was that the orbital height variation from 20 to 100 km requires a solution of a higher degree lunar gravity field at each bootstrapping step. The increased size of the field allow the model to follow high resolution gravity induced inter-satellite range measurements at altitudes below 30 km. For the higher resolution gravity fields, global low altitude coverage is needed, which was not obtained until the end of the primary mission. The bootstrapping process with increasing resolution gravity fields continued for the extended mission, where the twin spacecraft were flown at decreasing altitudes as low as 2 km above the lunar surface.

In the following sub-sections a summary of results will be presented illustrating the improvement in measurement residuals during the bootstrapping process. Furthermore, the improvement of the estimated gravity field solutions is illustrated using Ka range change residuals during the Ka-boresight calibration maneuvers and correlation of the gravity field with the lunar topography based on Lunar Reconnaissance Orbiter laser altimetry data.<sup>9</sup>

*DSN One-way and Two-way Doppler residuals* The DSN Doppler residuals are a direct measure of velocity errors of the spacecraft ephemerides and thus an excellent way to assess the orbit quality and by inference the gravity field quality. The Doppler residual results in this section are summarized from Fahnestock et al.<sup>10</sup> For the primary mission, the average magnitude of per-arc Root Mean Square (RMS) residuals for the DSN Doppler data progressed from  $\sim 0.7$  mm/s with our first orbits down to  $\sim 0.1$  mm/s with our orbits fit using the publicly released 420x420 gravity field. For the extended mission, the average and maximum magnitude of per-arc RMS residuals for the DSN Doppler data progressed from 1.6 and 13.7 mm/s, respectively, with orbits fit using the released 420x420 gravity field, down to  $\sim 0.7$  and  $\sim 2.5$  mm/s, respectively, with orbits fit using the best 660x660 gravity field available at the time of completion of the extended mission. The bootstrapping process, based on these results, has not yet converged and higher degree and order gravity fields need to be estimated to capture all the remaining gravity field modelling error in the

orbit ephemerides. This is particularly true for the low altitude phase of the extended mission.

*Orbit overlap residuals* As another metric of orbit determination quality and by inference the gravity field quality, for each spacecraft the RMS is calculated of the difference between adjacent and overlapping 36-hour arcs (centered at noon) in each Radial Transverse Normal (RTN) frame component of the spacecraft position. The RSS difference is computed based on 5 second samples over the central 10 hours of the nominal 12 hour overlap period. In this section the orbit overlap RMS results are summarized from Fahnstock et al.<sup>10</sup> For the primary mission, the orbit overlap metrics started out poorly, reaching up to 13 m, up to 230 m, and up to 260 m in radial, along-track, and cross-track, respectively. The same metrics improved to no more than 0.2 m, 2 m, and 0.7 m in radial, along-track, and cross-track, respectively, using the released 420x420 gravity field. For the extended mission, the same orbit overlap metrics went from up to 30 m in radial and cross-track and up to 150 m in along-track using the released 420x420 gravity field, down to no more than 5 m in radial and cross-track and no more than 25 m in along-track using the best 660x660 gravity field available at the time of completion of the extended mission. From these results it can be concluded that the bootstrapping process is not complete since the accuracy goal for spacecraft ephemerides is at the decimeter level. Higher degree and order fields need to be estimated to improve the orbit overlap statistics, particularly for the low altitude portion of the extended mission.

*Ka range rate residuals* In this section the evolution of the inter-satellite Ka range rate RMS residuals during the bootstrapping processing are summarized from Fahnstock et al.<sup>10</sup> For the primary mission, the average and maximum magnitude of per-arc RMS residuals for inter-satellite Ka range rate data progressed from  $\sim 20$  and  $\sim 83 \mu\text{m/s}$ , respectively, in the first bootstrapping iteration, down to  $\sim 0.3$  and  $\sim 1.9 \mu\text{m/s}$ , respectively, based on orbit determination using the publicly released 420x420 gravity field.<sup>2</sup> For the significantly different orbital geometry of the extended mission, the average and maximum magnitude of per-arc RMS residuals for inter-satellite Ka range rate data progressed from  $\sim 19$  and  $\sim 113 \mu\text{m/s}$ , respectively, with orbits fit using the same 420x420 gravity field, down to  $\sim 8$  and  $\sim 52 \mu\text{m/s}$ , respectively, with orbits fit using the best 660x660 gravity field available at the time of completion of the extended mission. From these results it is clear that the bootstrapping process is not complete and that higher degree and order gravity fields need to be estimated in order to fit the Ka range rate data at the level of  $\sim 0.03 \mu\text{m/s}$  data noise. This is particular true for low altitude data during the extended mission.

*Ka range rate time tag error solutions* The Ka range rate time tag error is estimated as part of the gravity field determination process to account for any timing error in the preprocessing of the science measurements and to provide consistency with the DSN Doppler tracking data. In this process the time tag errors are estimated as a constant offset per 36-hour orbit arc. In general Ka range rate time tag errors can not be completely separated from gravity error in the gravity field determination process, particularly for poor orbit geometries like the “face-on” geometry, where the normal component of the orbit plane is pointing towards Earth. The onboard time tags for the Ka range rate data are derived from a very stable clock, therefore the stability of the time tag error estimates is an indicator of remaining gravity errors of a particular gravity field solution. In this section the evolution of the Ka range rate time tag error are summarized from Fahnstock et al.<sup>10</sup> For the primary mission, the KBRR time tag bias estimate initially ranged between  $-30$  to  $+30$  milliseconds, and with the orbits fit using the public released 420x420 gravity field,<sup>2</sup> time tag error estimates varied by  $\sim 1$  millisecond about the mean value across all arcs. For the extended mission, the KBRR time tag bias estimate varied substantially during “face on” orbit geometries, reaching  $-26$  and  $+120$  milliseconds, with orbits fit using the public released 420x420 gravity

field. The KBRR time tag bias estimate variations dipped to  $\sim 2$  milliseconds about a shallowly rising trendline from 50.575 milliseconds (first arc) to 52.779 milliseconds (last arc), using the best 660x660 gravity field available at time of the completion of the extended mission. The conclusion for the Ka range rate time tag error estimate is that the bootstrapping processing has converged, given the observed stability of the solutions for the latest gravity field.

*Ka-boresight maneuver range change residuals* As stated before, the objective of the Ka-boresight calibration maneuvers is to estimate the Ka-boresight vector by combining observed range change minima during two  $3^\circ$  deg slews perpendicular to inter-spacecraft line of sight. During these maneuvers the total range change between the spacecraft is at the 1.5 km level while the range changes due to the spacecraft slews are only about 1.5 mm, as shown in Figure 7a. Therefore, the inter-satellite range signals due to orbit geometry and gravitation need to be removed from the total observed inter-satellite range in order to form the range change residuals needed for Ka-boresight estimation. The spacecraft slews are executed using momentum wheels, therefore no external force is imparted on the spacecraft during the maneuver. Thus the only signals in the inter-satellite range are due to orbit geometry, lunar gravity, and range changes induced by the spacecraft slews. As the spacecraft ephemerides and gravity field improve, the remaining range change residual should be due to the spacecraft slews. The remaining range change can then be used to assess the quality of the removed signals by checking how close the observed range change is to expected range change signal based on ground information for the Ka-boresight vector. In Figure 7a a good agreement can be seen between the computed range change residual and the observed range change after removal of the orbit geometry computed with a gravity field of degree 360. Figure 7b shows the evolution of the range change residual during the bootstrapping process and the clear improvement from bootstrapping, increasing the resolution of the gravity fields from degree and order 210 to 360.

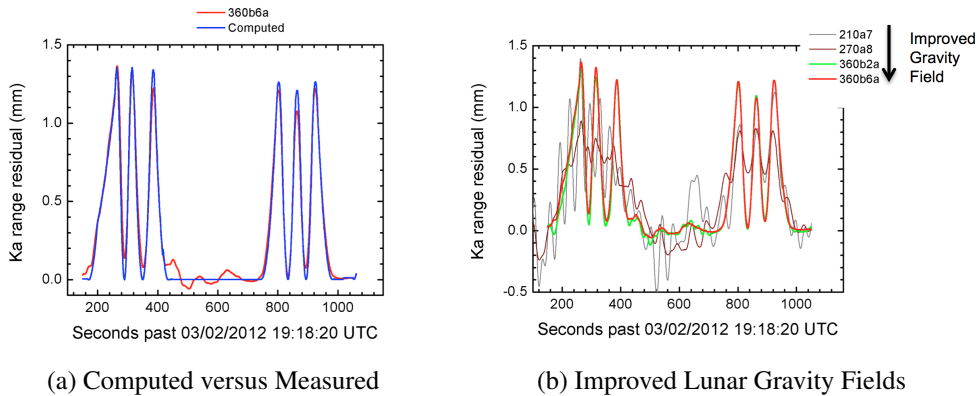


**Figure 7: Ka Boresight Maneuver Range Change Residuals**

*Gravity correlated with lunar topography results* Correlation of gravity anomalies with a gravity calculation based on the lunar topography derived from the Lunar reconnaissance Orbit (LRO) laser altimetry data<sup>2</sup> provides an independent check on the GRAIL observed lunar gravity field. The correlation between the topography derived gravity data and the GRAIL observed gravity field is expected to be high above degree 80. From the GRAIL data it was found that above degree 80, the spherical harmonic expansion was 98% correlated with the surface topograph.<sup>2</sup> During the bootstrapping process, which produced higher resolution lunar gravity fields, the 98% correlation extended to higher degrees with each iteration,<sup>1112</sup> which demonstrates that the gravity fields in the

bootstrapping process evolve to more physically accurate lunar gravity fields with each iteration.

## SUMMARY

A complete description was provided of the GRAIL gravity science measurements and the transformations needed to convert the measurements into the solar system barycentric frame required by the gravity field determination process. It was noted that nearly every transformation is a function of the accuracy of the spacecraft ephemerides and that with the available pre-flight lunar gravity fields the spacecraft ephemerides accuracy was insufficient for the lunar gravity field estimation. A bootstrapping strategy was developed, iterating between science data preprocessing and lunar gravity field determination to achieve the required transformation accuracy. Orbit determination played a pivotal role in the bootstrapping process, because of the aforementioned dependence of measurement transformations on the spacecraft ephemerides accuracy. The bootstrapping strategy was validated using a simulation, in which the truth lunar gravity field and supporting parameters were fully recovered. The bootstrapping strategy was applied to flight data and it was soon realized that because of the orbital altitude variation from 30 to 100 km in the primary mission, bootstrapping should include a steady increase in the resolution of the estimated gravity field. Although the bootstrapping process converged for the primary mission data, further bootstrapping with higher resolution fields is needed for the extended mission, where the orbital altitudes were as low as 2 km above the lunar surface.

## ACKNOWLEDGMENT

The authors constitute the GRAIL Science Data System (SDS) team, which is part of the GRAIL project and we want to acknowledge the excellent support received from the project during the mission planning and operations. We thank Wenwen Lu for her contributions to the bootstrapping process simulation. Furthermore, we thank Stephan Esterhuizen and Dong Shin for their excellent work on the TTS-DTE measurements. Finally, we thank Don Fleishman for providing radio science receiver observations of the radio science beacon on the GRAIL spacecraft.

This research was carried out at the Jet Propulsion Laboratory, California Institute of Technology, under a contract with the National Aeronautics and Space Administration. Reference herein to any specific commercial product, process or service by trade name, trademark, manufacturer, or otherwise, does not constitute or imply its endorsement by the United States Government or the Jet Propulsion Laboratory, California Institute of Technology.

©2013 California Institute of Technology. Government sponsorship acknowledged.

## REFERENCES

- [1] B. D. Tapley, S. Bettadpur, M. Watkins, and C. Reigber, "The gravity recovery and climate experiment: Mission overview and early results," *Geophys. Res. Lett.*, Vol. 31, May 2004, pp. 9607–+, 10.1029/2004GL019920.
- [2] M. T. Zuber, D. E. Smith, M. M. Watkins, S. W. Asmar, A. S. Konopliv, F. G. Lemoine, H. J. Melosh, G. A. Neumann, R. J. Phillips, S. C. Solomon, M. A. Wieczorek, J. G. Williams, S. J. Goossens, G. Kruijinga, E. Mazarico, R. S. Park, and D.-N. Yuan, "Gravity Field of the Moon from the Gravity Recovery and Interior Laboratory (GRAIL) Mission," *ScienceExpress*, 2012, Science DOI: 10.1126/science.1231507.
- [3] G. Kruijinga, W. Bertiger, and N. Harvey, "Timing of Science Data for the GRAIL mission," JPL D-75620, Jet Propulsion Laboratory, California Institute of Technology, Pasadena, 2012.

- [4] N. Harvey, E. Fahnestock, D. Kahan, A. Konopliv, G. Kruiizinga, K. Oudrhiri, M. Paik, D. Yuan, S. Asmar, and M. Watkins, "GRAIL Level-1 Algorithm Theoretical Basis Document," JPL D-75862, Jet Propulsion Laboratory, California Institute of Technology, Pasadena, 2012.
- [5] S. Esterhuizen, "Moon-To-Earth: Eavesdropping on the GRAIL inter-spacecraft time-transfer link using a large antenna and a software receiver," *ION GNSS*, ION, 2012.
- [6] T. Moyer, "Formulation for Observed and Computed Values of Deep Space Network Data Types for Navigation," deep space communications and navigation series monograph 2, Jet Propulsion Laboratory, California Institute of Technology, Pasadena, 2000.
- [7] A. Konopliv, S. Asmar, E. Carranza, W. L. Sjogren, and D. N. Yuan, "Recent gravity models as a result of the lunar prospector mission," *Icarus*, Vol. 150, 2001, pp. 1–18, 10.1006/icar.2000.6573.
- [8] E. Carranza, A. Konopliv, and M. Ryne, "Lunar Prospector Orbit Determination Uncertainties Using the High Resolution Lunar Gravity Models," AIAA paper AAS 99-325 presented at AAS/AIAA Astrodynamics Specialists Conference, Girdwood, Alaska , 16-19 August, 1999.
- [9] D. E. Smith, M. T. Zuber, G. A. Neumann, F. G. Lemoine<sup>2</sup>, E. Mazarico, M. H. Torrence, J. F. McGarry, D. D. Rowlands, J. W. H. Ill, T. H. Duxbury, O. Aharonson, P. G. Lucey, M. S. Robinson, O. S. Barnouin, J. F. Cavanaugh, X. Sun, P. Liiva, D. d. Mao<sup>11</sup>, J. C. Smith, and A. E. Bartels, "Initial Observations from the Lunar Orbiter Laser Altimeter (LOLA)," *Geophys. Res. Lett.*, 2010, 10.1029/2010GL043751.
- [10] E. Fahnestock, S. Asmar, N. Harvey, D. Kahan, A. Konopliv, G. Kruiizinga, K. Oudrhiri, M. Paik, R. Park, D. Strelakov, and D. Yuan, "GRAIL Science Data System Orbit Determination: Approach, Strategy, and Performance," AIAA paper AAS 13-271 presented at AAS/AIAA Spaceflight Mechanics Meeting, Lihue, Hawaii , 11-14 Februari, 2013.
- [11] A. Konopliv, R. Park, D. Yuan, S. Asmar, M. Watkins, J. Williams, E. Fahnestock, G. K. M. Paik, D. Strelakov, H. Nate, D. Smith, and M. Zuber, "The JPL Lunar Gravity Field to degree 660 from the GRAIL Primary Mission," Submitted to Journal of Geophysical Research January, 2013.
- [12] R. Park, A. Konopliv, D. Yuan, S. Asmar, E. Fahnestock, G. Kruiizinga, M. Paik, M. Watkins, D. Smith, and M. Zuber, "High-Resolution Lunar Gravity from the Gravity Recovery And Interior Laboratory Mission," AIAA paper AAS 13-272 presented at AAS/AIAA Spaceflight Mechanics Meeting, Lihue, Hawaii , 11-14 February, 2013.